

Induction Motor Control with Predicted Maximum Electromagnetic Torque and Speed

Nicoleta Roxana BUZATU, Dimitrie ALEXA, Georgian Alexandru LAZAR, Dan BUTNICU,
Oana Loredana BUZATU

Technical University "Gheorghe Asachi" of Iasi, Bd. Carol I, nr 11, RO-700506 Iasi, Romania
rbuzatu@etc.tuiasi.ro

Abstract — The paper presents a new control of an induction motor, based on the indirect rotor – flux – oriented control (IRFOC). The control circuit ensures an independent electromagnetic torque control, which limits its maximum value to a predicted one. The torque predicted values are dependent on the external parameters of the induction motor and overrides the speed control. The proposed system can be implemented in various applications constrained by mechanical or physical factors, which require variable torque and speed.

Index Terms — Indirect Rotor – Flux – Oriented Control (IRFOC), induction motor, rotor, torque, speed

I. INTRODUCTION

The control of induction machines and drives has been highly developed in recent years. Induction generators have been widely used for wind power generation. Induction motors have been the workhorses in industry for variable speed applications in a wide power range. There are a number of significant control methods available for induction motors including scalar control, vector or field-oriented control, direct torque and flux control, and adaptive control [1]. Scalar control is aimed at controlling the induction machine to operate at a steady state, by varying the amplitude and frequency of the fundamental supply voltage [2]. A method which provides an improved V/f control for high voltage induction motors was proposed in [3]. The scalar controlled drive, in contrast to a vector or field-oriented controlled one, is easier to implement, but provides somewhat inferior performance. This control method ensures limited speed accuracy, especially in the low speed range and poor dynamic torque response.

The concept of vector control was suggested by Hasse in 1969 and Blaschke in 1972 [4]. In the indirect method of orientation, the flux is estimated from motor inverse dynamics, and one of the three basic implementation schemes based on stator-flux, air gap-flux, or rotor - flux orientations can be used [5].

Furthermore, in literature various efficient methods of induction motor torque control are presented [1 – 7]. These methods target a precise operating speed control, ensuring larger acceleration while maintaining a small ripple.

The control of the maximum generated output power is influenced both by the parameters of the motor and of the converter. In many applications such as cable railway, electric powered machines that operate on slippery surfaces, mine carts or elevators used in construction yards there is the necessity of limiting the motor operating speed. This requirement is due to either the derail danger (mine carts),

the malfunction of the pulleys (elevator) or adherence loss. The solution that solves the above mentioned problems is to limit not only the speed of the motor, but also the torque. The maximum values for these parameters can be computed as referred to the output load of the motor and the characteristics of the equipment that contains the motor.

In this paper the control of the motor using the IRFOC method was employed [6 – 9]. The novelty of the proposed method is the use of a single regulator, which controls not only the speed of the motor, but also the maximum value of the torque. This method is preferred due to the simplicity of the equations that generate the regulation schemes. Another major advantage of the IRFOC is the improved dynamical performance in case of low speed.

II. INDUCTION MOTOR AND THE EXPRESSION OF THE ELECTROMAGNETIC TORQUE

The modeling of the induction motor with the rotor in short – circuit connection can be made starting from the voltage equations of the three phases (x, y, z) of the stator and rotor [2], [10]:

$$u_{sk}(t) = R_s i_{sk}(t) + \frac{d\Psi_{sk}(t)}{dt} \quad (1 a)$$

$$u_{rk}(t) = R_r i_{rk}(t) + \frac{d\Psi_{rk}(t)}{dt} = 0 \quad (1 b)$$

where k can be x, y or z. The measures $\{u_{sk}(t), i_{sk}(t), \Psi_{sk}(t)\}$, $\{u_{rk}(t), i_{rk}(t), \Psi_{rk}(t)\}$, represent the instantaneous values of the voltages, currents and total fluxes through the stator and rotor, respectively.

Three bi-dimensional coordinate systems can be defined: $q_s - d_s$ (containing the stator), $q_r - d_r$ (containing the rotor) and $q_\phi - d_\phi$ (containing the rotor's flux). The relative positions of these reference coordinate systems are presented in Fig. 1.

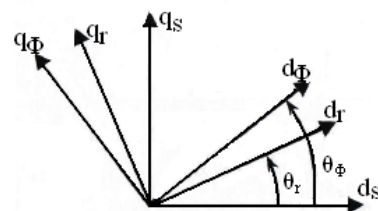


Figure 1. Phasor transformation diagram of the rotor, stator and flux measures

The angle θ_r depends on the relative position of the system ($q_r - d_r$) as referred to the fixed system $q_s - d_s$. The angular velocity of the rotor as referred to the stator is

defined as:

$$\omega_r = \frac{d\theta_r}{dt} \quad (2 \text{ a})$$

The angle θ_Φ determines the relative position of the system ($q_\Phi - d_\Phi$) as referred to the stator. In this case the angular velocity of the rotor's flux vector with respect to the stator is:

$$\omega_\Phi = \frac{d\theta_\Phi}{dt} \quad (2 \text{ b})$$

After using the operator:

$$a = e^{j\frac{2\pi}{3}} \quad (3)$$

The voltages, currents and fluxes expressed in equations (1 a) and (1 b) can be represented in a vectorial form with the help of the either $q_s - d_s$ or $q_r - d_r$ coordinates.

$$\left\{ \begin{aligned} \underline{u}_s^{(s)} &= \frac{2}{3} [u_{sx}(t) + au_{sy}(t) + a^2u_{sz}(t)] \\ &= u_{s(ds)} + ju_{s(qs)} \\ \underline{i}_s^{(s)} &= \frac{2}{3} [i_{sx}(t) + ai_{sy}(t) + a^2i_{sz}(t)] \\ &= i_{s(ds)} + ji_{s(qs)} \\ \underline{\Psi}_s^{(s)} &= \frac{2}{3} [\Psi_{sx}(t) + a\Psi_{sy}(t) + a^2\Psi_{sz}(t)] \\ &= \Psi_{s(ds)} + j\Psi_{s(qs)} = L_s \underline{i}_s^{(s)} + L_m \underline{i}_r^{(s)} \end{aligned} \right. \quad (4)$$

and

$$\left\{ \begin{aligned} \underline{u}_r^{(r)} &= \frac{2}{3} [u_{rx}(t) + au_{ry}(t) + a^2u_{rz}(t)] \\ &= u_{r(dr)} + ju_{r(qr)} \\ \underline{i}_r^{(r)} &= \frac{2}{3} [i_{rx}(t) + ai_{ry}(t) + a^2i_{rz}(t)] \\ &= i_{r(dr)} + ji_{r(qr)} \\ \underline{\Psi}_r^{(r)} &= \frac{2}{3} [\Psi_{rx}(t) + a\Psi_{ry}(t) + a^2\Psi_{rz}(t)] \\ &= \Psi_{r(dr)} + j\Psi_{r(qr)} = L_r \underline{i}_r^{(r)} + L_m \underline{i}_s^{(r)} \end{aligned} \right. \quad (5)$$

where $\underline{i}_r^{(s)} = \underline{i}_r^{(r)} e^{j\theta_r}$, $\underline{i}_s^{(r)} = \underline{i}_s^{(s)} e^{-j\theta_r}$.

Rearranging equations (1 a) and (1 b) with the vectorial notations form equations (4) and (5), the following expressions are obtained:

$$\left\{ \begin{aligned} \underline{u}_s^{(s)} &= R_s \underline{i}_s^{(s)} + \frac{d\Psi_s^{(s)}}{dt} \\ \underline{u}_r^{(r)} &= R_r \underline{i}_r^{(r)} + \frac{d\Psi_r^{(r)}}{dt} \end{aligned} \right. \quad (6)$$

From relation (2 a), the value of $u_r^{(r)}$ (equation 6) can be written with respect to the $q_s - d_s$ coordinates (which contain the stator). With the help of relations (4) and (5), the following equation is deduced:

$$\left\{ \begin{aligned} \underline{u}_s^{(s)} &= R_s \underline{i}_s^{(s)} + \frac{d}{dt} (L_s \underline{i}_s^{(s)} + L_m \underline{i}_r^{(s)}) \\ \underline{u}_r^{(s)} = 0 &= R_r \underline{i}_r^{(s)} + \frac{d}{dt} (L_m \underline{i}_s^{(s)} + L_r \underline{i}_r^{(s)}) - \\ &\quad - j\omega_r (L_m \underline{i}_s^{(s)} + L_r \underline{i}_r^{(s)}) \end{aligned} \right. \quad (7)$$

The corresponding expressions that describe the operation of the induction motor used in the simulations are obtained after rearranging equation (7) as referred to the coordinate system $q_s - d_s$. Furthermore, this equation is appended with the equation that describes the mechanical operation of the system.

$$\frac{d\omega_r}{dt} = \frac{1}{J} \left[\frac{2}{3} p L_m (i_{s(qs)} i_{r(ds)} - i_{s(ds)} i_{r(qs)}) - M_s \right] \quad (8)$$

where M_s is the total static torque of the motor shaft and J is the total inertial momentum of the motor shaft, L_s is the stators inductance, L_r is the rotors inductance, L_m is the magnetizing inductance and p is the number of poles.

III. THE CONTROL SYSTEM

The control circuit illustrated in Fig. 2 employs the use of the IRFOC vectorial method for driving the induction motor [2]. The control of the maximum torque is achieved through the TC, IDΦM, TE and CS blocks, which are depicted in Fig. 2 and are presented in this section. An essential remark is that the circuit needs just one speed regulator, without an employing a second torque regulator.

The expression of the electromagnetical torque m_e is shown in equation (9):

$$\underline{m}_e = -\frac{3}{2} p \underline{\Psi}_r^\Omega \times \underline{i}_r^\Omega \quad (9)$$

where p – represent the number of poles,

From this equation, it can be concluded that the electromagnetical torque is insensitive to the rotational system $q_\Omega - d_\Omega$ in which the vectors $\underline{\Psi}_r$ and \underline{i}_r are expressed. On this ground, the system $q_\Phi - d_\Phi$ (containing the magnetic flux of the rotor) can be selected, without influencing the electromagnetical torque. In this coordinate system the $\underline{\Psi}_r^{(\Phi)}$ vector is fixed because the chosen system $q_\Phi - d_\Phi$ contains this vector. The optimal operation is obtained provided that the $\underline{\Psi}_r^{(\Phi)}$ vector is oriented along the $d\Phi$ axis and has a constant value smaller than the saturation value of the machine. In this situation, the magnetization current i_{mr} is constant $\left(\frac{di_{mr}}{dt} = 0 \right)$. Considering equation (7), the

coordinate transformation and the fact that the voltage of the rotor is zero (the motor has the rotor in a short – circuit connection), then equation (9) is equivalent to:

$$|m_e| = \frac{2}{3} p \frac{L_m^2}{L_r} i_{s(d\Phi)} i_{s(q\Phi)} \quad (10)$$

Matlab simulations are depicted in Table 1.

TABLE I. PARAMETERS OF THE INDUCTION MOTOR

Parameter	Value
Output power	$P_N = 2.2 \text{ kW}$
Stator resistance	$R_s = 1.8 \Omega$
Rotor resistance	$R_r = 1.93 \Omega$
Stator and rotor inductance	$L_s = L_r = 0.02 \text{ H}$
Number of pole pairs	$p = 2$
Motor inertia	$J = 0.21 \text{ Kg}\cdot\text{m}^2$
Constant friction torque	$K = 0.074$
Magnetizing inductance	$L_m = 0.3 \text{ H}$

For each simulation scenario a set of maximum speed (ω_M) and maximum torque (T_M) were defined. The values assigned to these two variables are time dependent. In case of a practical application setting, the system allows flexibility, as the time axis can be changed into a space (distance) axis, depending on the specific task requirement.

In Fig. 3a and Fig. 4a, the maximum predicted values for speed and torque are plotted.

In the simulation illustrated in Fig. 3, the maximum torque T_M is that which limits the dynamic behavior of the motor. Starting from point $t = 1.5 \text{ s}$, the torque is step decreased and it can be seen in Fig. 3b that not only the electromagnetic torque follows this step variation but also the acceleration of the motor is decreased as well. Another important remark is that for all the simulation period the speed never equals the maximum admissible value ω_M . The electromagnetic torque (Fig. 3b) respects the maximum imposed value from Fig. 3a. The current of the stator (Fig. 3c) has two different constant values corresponding to the two torque values.

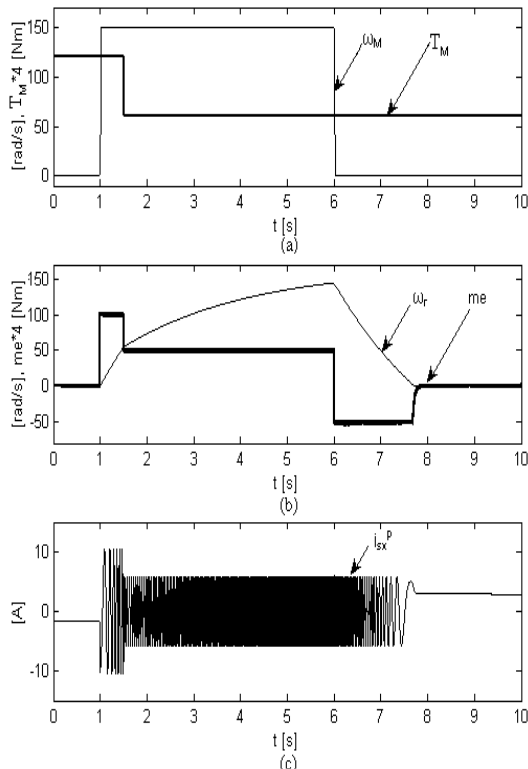


Figure 3. a) Simulation results of the predicted speed and electromagnetic torque; b) Simulation results of the speed and electromagnetic torque response of the induction motor; c) Waveform of the stator's phase current.

In the simulations depicted in Fig. 4, the speed of the induction motor equals the defined maximum value plotted

in Fig. 4a at point $t = 1.8 \text{ s}$. From this point to time $t = 2.5 \text{ s}$, the speed is the parameter which limits the dynamic behavior of the motor. As a consequence, the electromagnetic torque step decreases in this time frame down to a value that is able to respect the defined motor's speed. In the time moment $t = 2.5 \text{ s}$, the defined maximum torque T_M (Fig. 4a) is step decreased. The new torque value is not able to comply to the maximum admissible speed anymore. From this point, the torque is the parameter which limits the dynamic behavior of the motor. The current of the stator has three distinct values (Fig. 4c) associated to the three electromagnetic torques depicted in Fig. 4b.

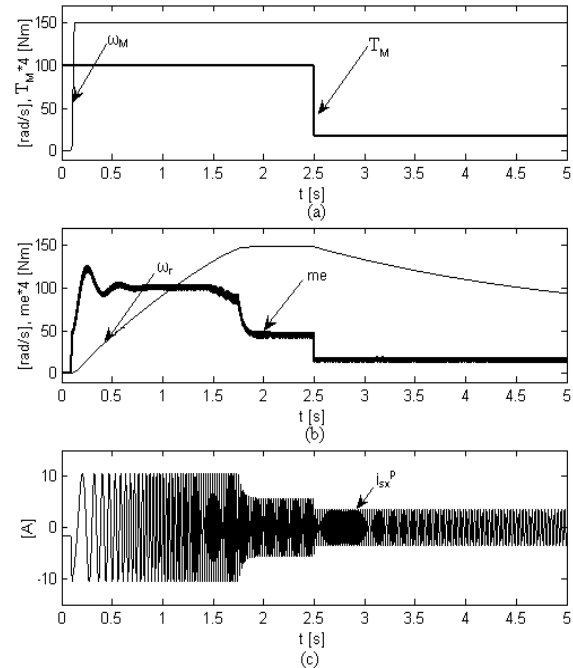


Figure 4. a) Simulation results of the predicted speed and electromagnetic torque; b) Simulation results of the speed and electromagnetic torque response of the induction motor; c) Waveform of the stator's phase current.

V. CONCLUSION

This paper presents a new induction motor control circuit designed to limit the speed or/and the electromagnetic torque according to the maximum desired values. The performed simulations confirm these demands. The proposed drive circuit differs from the standard ones through the use of just one speed regulator, without an additional torque regulator. The control of the torque is done indirectly through speed limitation, so that the resulting torque is smaller than the maximum prescribed value, while the magnetization current (i_{mr}) remains constant. For each time sequence both the maximum speed ω_M and the maximum torque T_M are predicted. These values can be automatically computed depending on the weight, but this task is beyond the scope of this paper. The only concern of the user is to control the start of the machine.

A similar matter appears in case of the construction yard elevators or any other application in which both speed and maximum torque have to be defined in distinct sequences of the trajectory.

REFERENCES

- [1] B. K. Bose, "Modern Power Electronics and AC Drives", Pearson Education, Inc., 2002.
- [2] Carlos A. Martins, Adriano S. Carvalho, "Technological Trends in Induction Motor Electrical Drives", IEEE Porto Power Tech Conference, vol. 2, Sep. 2001.
- [3] L. Ben-Brahim, "Improvement of the stability of the V/f controlled induction motor drive systems", IEEE Proceedings of the 24th Annual Conference, vol. 2, pp. 859-864, 1998.
- [4] F. Blaschke, "The principle of Field Orientation as Applied to the New Transvektor Closed – Loop Control System for Rotating – Field Machines", IEEE Press, New York, 1981.
- [5] P. de Wit, Romeo Ortega, Iven Mareels, "Indirect Field Oriented Control of Induction Motors is Robustly Globally Stable", IEEE conference on Decision and Control, vol. 3, pp. 2139 - 2144, 1995.
- [6] Sahoo S.K. Panda, S.K. Jian-Xin Xu, "Indirect torque control of switched reluctance motors using iterative learning control" Power Electronics, IEEE Transactions on , vol. 20, Issue 1, pp. 200 – 208, Jan 2005.
- [7] Yu Zhang, Zhenhua Jiang, "Indirect Field-Oriented Control of Induction Machines Based on Synergetic Control Theory", Power and Energy Society General Meeting - Conversion and Delivery of Electrical Energy in the 21st Century, 2008 IEEE, pp. 1 – 7, 2008.
- [8] Leonhard W., "Control of Electrical Drives", Springer - Verlag, Berlin, 1985
- [9] Birou I., Maier V., Pavel S., Rusu, C., "Indirect Vector Control of an Induction Motor with Fuzzy-Logic based Speed Controller", Advances in Electrical and Computer Engineering, vol.1, pp.116 -120, 2010.
- [10] Kelemen A., Imecs M., "Vector Control of Induction Machine Drives", Vol.1, OMIKK Publisher, Budapest, 1991